

Coupled Superconducting and Magnetic Order in CeCoIn₅

M. Kenzelmann *et al.*
Science **321**, 1652 (2008);
DOI: 10.1126/science.1161818

This copy is for your personal, non-commercial use only.

If you wish to distribute this article to others, you can order high-quality copies for your colleagues, clients, or customers by [clicking here](#).

Permission to republish or repurpose articles or portions of articles can be obtained by following the guidelines [here](#).

The following resources related to this article are available online at www.sciencemag.org (this information is current as of June 28, 2014):

Updated information and services, including high-resolution figures, can be found in the online version of this article at:

<http://www.sciencemag.org/content/321/5896/1652.full.html>

Supporting Online Material can be found at:

<http://www.sciencemag.org/content/suppl/2008/08/21/1161818.DC1.html>

This article **cites 22 articles**, 1 of which can be accessed free:

<http://www.sciencemag.org/content/321/5896/1652.full.html#ref-list-1>

This article has been **cited by** 31 article(s) on the ISI Web of Science

This article has been **cited by** 3 articles hosted by HighWire Press; see:

<http://www.sciencemag.org/content/321/5896/1652.full.html#related-urls>

This article appears in the following **subject collections**:

Physics

<http://www.sciencemag.org/cgi/collection/physics>

References and Notes

1. G. Grüner, *Density Waves in Solids*, vol. 89 of *Frontiers in Physics* (Addison-Wesley, Reading, MA, 1994).
2. V. Brouet *et al.*, *Phys. Rev. Lett.* **93**, 126405 (2004).
3. V. Brouet *et al.*, *Phys. Rev. B* **77**, 235104 (2008).
4. E. DiMasi, M. C. Aronson, J. F. Mansfield, B. Foran, S. Lee, *Phys. Rev. B* **52**, 14516 (1995).
5. G.-H. Gweon *et al.*, *Phys. Rev. Lett.* **81**, 886 (1998).
6. A. Fang, N. Ru, I. R. Fisher, A. Kapitulnik, *Phys. Rev. Lett.* **99**, 046401 (2007).
7. C. Malliakas, S. Billinge, H. Kim, M. Kanatzidis, *J. Am. Chem. Soc.* **127**, 6510 (2005).
8. N. Ru *et al.*, *Phys. Rev. B* **77**, 035114 (2008).
9. P. B. Littlewood, C. M. Varma, *Phys. Rev. B* **26**, 4883 (1982).
10. R. Sooryakumar, M. V. Klein, *Phys. Rev. B* **23**, 3213 (1981).
11. Materials and methods are available as supporting material on *Science* Online.
12. J. Laverock *et al.*, *Phys. Rev. B* **71**, 085114 (2005).
13. W. S. Fann, R. Storz, H. W. K. Tom, J. Bokor, *Phys. Rev. B* **46**, 13592 (1992).
14. M. Lisowski *et al.*, *Appl. Phys. A* **78**, 165 (2004).
15. U. Bovensiepen, *J. Phys. Condens. Matter* **19**, 083201 (2007).
16. L. Perfetti *et al.*, *Phys. Rev. Lett.* **97**, 067402 (2006).
17. P. A. Loukakos *et al.*, *Phys. Rev. Lett.* **98**, 097401 (2007).
18. D. M. Fritz *et al.*, *Science* **315**, 633 (2007).
19. P. Baum, D.-S. Yang, A. H. Zewail, *Science* **318**, 788 (2007).
20. C. v. Korff Schmising *et al.*, *Phys. Rev. Lett.* **98**, 257601 (2007).
21. J. Demsar, K. Biljaković, D. Mihailovic, *Phys. Rev. Lett.* **83**, 800 (1999).
22. A. Cavalleri, T. Dekorsy, H. H. W. Chong, J. C. Kieffer, R. W. Schoenlein, *Phys. Rev. B* **70**, 161102 (2004).
23. M. Chollet *et al.*, *Science* **307**, 86 (2005).
24. B. Rethfeld, A. Kaiser, M. Vicanek, G. Simon, *Phys. Rev. B* **65**, 214303 (2002).
25. T. Dekorsy, G. C. Cho, H. Kurz, *Coherent Phonons in Condensed Media*, vol. 76 of *Springer Topics in Applied Physics* (Springer, Berlin, 2000).
26. M. Lavagnini *et al.*, preprint available at <http://arxiv.org/abs/0806.1455v1> (2008).
27. G. Travaglini, L. Mörke, P. Wachter, *Solid State Commun.* **45**, 289 (1983).
28. R. V. Yusupov *et al.*, preprint available at <http://arxiv.org/abs/0807.1022v1> (2008).

29. A. Damascelli, Z. Hussain, Z.-X. Shen, *Rev. Mod. Phys.* **75**, 473 (2003).
30. We thank L. DeGiorgi *et al.* and D. Mihailovic *et al.* for fruitful discussions. We acknowledge funding from the Max-Planck-Gesellschaft through the International Max Planck Research School and by the Deutsche Forschungsgemeinschaft through BO 1823/2, Sfb 450, and the Heisenberg program. This work is supported by the U.S. Department of Energy Office of Basic Energy Science, Division of Materials Science and Engineering.

Supporting Online Material

www.sciencemag.org/cgi/content/full/1160778/DC1

Materials and Methods

SOM Text

Figs. S1 to S5

References

Movie S1

21 May 2008; accepted 1 August 2008

Published online 14 August 2008;

10.1126/science.1160778

Include this information when citing this paper.

Coupled Superconducting and Magnetic Order in CeCoIn₅

M. Kenzelmann,^{1,2} Th. Strässle,³ C. Niedermayer,³ M. Sigrist,⁴ B. Padmanabhan,³ M. Zolliker,¹ A. D. Bianchi,⁵ R. Movshovich,⁶ E. D. Bauer,⁶ J. L. Sarrao,⁶ J. D. Thompson⁶

Strong magnetic fluctuations can provide a coupling mechanism for electrons that leads to unconventional superconductivity. Magnetic order and superconductivity have been found to coexist in a number of magnetically mediated superconductors, but these order parameters generally compete. We report that close to the upper critical field, CeCoIn₅ adopts a multicomponent ground state that simultaneously carries cooperating magnetic and superconducting orders. Suppressing superconductivity in a first-order transition at the upper critical field leads to the simultaneous collapse of the magnetic order, showing that superconductivity is necessary for the magnetic order. A symmetry analysis of the coupling between the magnetic order and the superconducting gap function suggests a form of superconductivity that is associated with a nonvanishing momentum.

CeCoIn₅ is a clean ambient-pressure d-wave superconductor (¹) and crystallizes in a tetragonal structure (Fig. 1). Because of its proximity to a magnetic quantum critical point, it features strong antiferromagnetic correlations that result in an enhancement of the effective electronic mass and heavy-fermion behavior (²). However, CeCoIn₅ undergoes a transition to superconductivity before magnetic order can be established (², ³). The superconducting gap function has probably a d_{x2-y2} symmetry (⁴⁻⁷), and it is generally believed that superconductivity in CeCoIn₅ is mediated by magnetic fluctuations. The Fermi surface is strongly two-dimensional (⁸, ⁹), and superconductivity in an applied field is Pauli-limited (¹⁰), that is, it is destroyed by a coupling of external magnetic

fields to the spins of the Cooper pairs and not by orbital depairing. CeCoIn₅ features an unusual field-temperature (H-T) phase diagram (¹¹, ¹²): below $T_0 = 0.31$ $T_c = 1.1$ K (T_c , critical temperature), the transition from the normal to the superconducting state is first-order (¹⁰, ¹¹). Further, there is evidence for a second superconducting phase, the “Q phase,” which exists only when $T < 0.3$ K and with high fields close to the upper critical field (¹¹, ¹³, ¹⁴). It has been suggested (¹¹, ¹⁵) that this high-field phase may represent a superconducting phase that was proposed by Fulde, Ferrell, Larkin, and Ovchinnikov (FFLO) and that carries a finite momentum as a result of the Zeeman splitting of the electron bands (¹⁶, ¹⁷).

A rich interplay between magnetic order and superconductivity is characteristic of heavy-fermion superconductors, with either magnetic order preceding the onset of superconductivity or superconductivity occurring in the vicinity of a quantum critical point (¹⁸, ¹⁹). Superconductivity in CeCoIn₅ is special in that it occurs close to a magnetic quantum critical point, but so far there has been no direct evidence of long-range magnetic order anywhere in the H-T phase diagram (²). However, there is microscopic evidence from nuclear magnetic resonance (NMR) measurements

for field-induced magnetism for high fields ($\sim H = 11$ T) in the tetragonal plane and for temperatures below which the $H_{c2}(T)$ phase boundary becomes first-order (H_{c2} , upper critical field) (²⁰). The NMR results were interpreted as evidence that the Q phase is a phase in which superconductivity and magnetic order coexist, but the character of the superconducting state could not be ascertained.

We used high-field neutron diffraction to directly search for magnetic Bragg peaks within the Q phase. The measurements were done at low temperatures and the field was applied along the crystallographic [1-10] direction in the tetragonal basal plane. For this field direction, the upper critical field in the zero-temperature limit is $H_{c2}(0) = 11.4$ T. The neutron diffraction data for wave-vectors along the (h, h, 0.5) reciprocal direction is shown in Fig. 2. Here, h represents the wave-vector transfer along either the [100] or the [010] direction in reciprocal lattice units (r.l.u.). When $10.5 \text{ T} < H < 11.4 \text{ T}$, neutron scattering provides clear evidence of Bragg peaks that arise from a magnetic structure that is modulated with the ordering wave-vector $\mathbf{Q} = (q, q, 0.5)$ (²¹) and that are present at neither higher nor lower fields outside of the Q phase (hence its name). Here, q represents the wave-vector for which the magnetic Bragg peak has most intensity and indicates the modulation of the magnetic structure along the a and b axes. The width of the peaks is resolution-limited, so the magnetic order extends over a length scale $\xi > 60$ nm. This is much larger than the diameter of vortex cores, which is of the order of the coherence length $\xi_0 \sim 10$ nm (⁵), and so magnetic order is not limited to the vortex cores.

The field and temperature dependence of the peak intensity of the $\mathbf{Q} = (q, q, 0.5)$ magnetic Bragg peak obtained from a fit to a Gaussian line shape is shown in Fig. 2. The magnetic order at $T = 60$ mK has a gradual onset with increasing field and collapses at the superconducting phase boundary H_{c2} in a first-order transition (Fig. 3A). The intensity of the magnetic Bragg peak can also be suppressed by increasing the temperature (Fig.

¹Laboratory for Developments and Methods, Paul Scherrer Institute, CH-5232 Villigen, Switzerland. ²Laboratory for Solid State Physics, Eidgenössische Technische Hochschule (ETH) Zurich, CH-8093 Zurich, Switzerland. ³Laboratory for Neutron Scattering, ETH Zurich, and Paul Scherrer Institute, CH-5232 Villigen, Switzerland. ⁴Institut für Theoretische Physik, ETH Zurich, CH-8093 Zurich, Switzerland. ⁵Département de Physique et Regroupement Québécois sur les Matériaux de Pointe, Université de Montréal, Montréal, Québec H3C 3J7, Canada. ⁶Condensed Matter and Thermal Physics, Los Alamos National Laboratory, Los Alamos, NM 87545, USA.

3B); the signal disappears at the same temperature at which specific heat measurements show evidence of a second-order phase transition (11). The neutron data suggest a transition that is second-order in temperature but first-order in field. The incommensuration q of the Bragg peak position is not field-dependent, as can be seen in the inset of Fig. 3A. The H - T phase diagram (Fig. 1) shows that magnetic order exists only in the superconducting \mathbf{Q} phase and not in the normal phase, which demonstrates that superconductivity is essential for magnetic order. Our results provide evidence that the ground state in this field and temperature range in the vicinity of $H_{c2}(0)$ has a multicomponent order parameter that directly couples superconductivity and magnetism. This type of order is at least partly due to strong antiferromagnetic fluctuations, arising from the proximity to a magnetic quantum critical point in CeCoIn₅.

Our experiment shows that the magnetic structure is a transverse amplitude-modulated incommensurate spin-density wave whose magnetic moments are orientated along the tetragonal c axis, modulated with the incommensurate wave-vector $(q, q, 0.5)$ perpendicular to the magnetic field. Neighboring Ce³⁺ magnetic moments that are separated by a unit cell lattice translation along the c axis are antiparallel (Fig. 1). The amplitude of the magnetic moment (m) at $T = 60$ mK and $H = 11$ T of $m = 0.15(5)$ Bohr magnetons (μ_B) is considerably smaller than expected for the Ce³⁺ free ion, possibly due to the Kondo effect. The direction of the ordered magnetic moment is consistent with magnetic susceptibility measurements (1) that identify the c axis as the easy axis, and it is also consistent with zero-field inelastic neutron measurements in which strong antiferromagnetic fluctuations have been observed that are polarized along the c axis (22).

The magnetic structure that satisfies NMR data (20) was described by an ordering wave-vector $\mathbf{Q} = (q, 0.5, 0.5)$ with unspecified q and the ordered magnetic moment along the applied field that was along the [100] direction. Our neutron measurements of field along the [1–10] direction reveal a magnetic order for which both the ordering wave-vector $\mathbf{Q} = (q, q, 0.5)$ and the ordered moments are perpendicular to the applied magnetic field, in contrast to the NMR data. This difference suggests that the direction of the incommensurate modulation \mathbf{Q} depends on the field direction, and that the order wave vector can be tuned with a rotation of the magnetic field in the basal plane. Finally, the absence of magnetic Bragg peaks at $H = 11$ T when $T > 0.3$ K confirms the interpretation of the NMR measurements (20) that the fluctuations for $0.3 \text{ K} < T < T_0$ are short-ranged and possibly only present inside the vortex cores.

The observation that magnetism exists only in the presence of superconductivity is in stark contrast to other materials in which long-range magnetic order and superconductivity merely coexist for a small magnetic field or pressure range because of their different origins (18, 19). Because no magnetic order is observed in CeCoIn₅

above the upper critical field H_{c2} , the relation between magnetic order and superconductivity is fundamentally different and cannot be seen as a competition. Instead, it appears that CeCoIn₅ in fields greater than H_{c2} gives rise to strong antiferromagnetic fluctuations that condense into magnetic order with decreasing magnetic field only through the opening of an electronic gap and

restructuring of the Fermi surface at the superconducting phase boundary. This means that the second-order magnetic quantum phase transition is inaccessible because, in its proximity, there is no energy scale associated with the antiferromagnetic fluctuations, and the superconducting energy gap becomes the dominant energy scale and determines the magnetic ground-state properties.

Fig. 1. H - T phase diagram of CeCoIn₅ with the magnetically ordered phase indicated by the red shaded area. The blue and open circles indicate a first- and second-order transition measured by specific heat (11), respectively, separating the superconducting from the normal phase. The green circles indicate a second-order phase transition inside the superconducting phase (11), and the red circles indicate the onset of magnetic order as measured in our experiment, showing that the magnetic order only exists in the \mathbf{Q} phase. (Inset) Magnetic structure of CeCoIn₅ at $T = 60$ mK and $H = 11$ T. The red arrows show the direction of the static magnetic moments located on Ce³⁺, and the yellow and blue circles indicate the position of the In and Co ions. The depicted structure does not include a possible uniform magnetization along the magnetic field direction. The solid red line indicates the amplitude of the Ce³⁺ magnetic moment along the c axis, projected on the (h, h, l) plane.

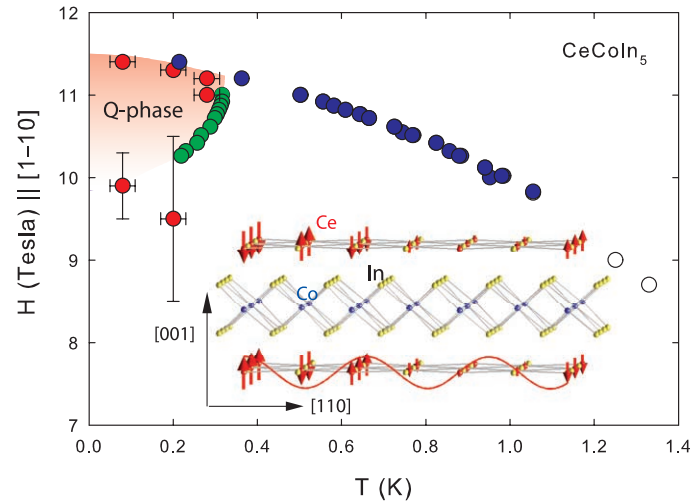


Fig. 2. The solid circles represent the neutron-scattering intensity at $T = 60$ mK for wave vectors $(h, h, 0.5)$ as a function of h for different fields as observed in the center channel of the position-sensitive detector (psd), showing the presence of a magnetic neutron diffraction peak at $(1 - q, 1 - q, 0.5)$ with $q = 0.44$ for (A) $H = 10.6$ T, (B) $H = 10.8$ T, (C) $H = 11$ T, and (D) $H = 11.3$ T. The gray circles in (A) and (B) represent the best estimate of the background, whereas they represent the neutron scattering intensity in (C) at $H = 11$ T and $T = 400$ mK and in (D) at $H = 11.4$ T and $T = 60$ mK. The solid red lines are fits of a Gaussian function to the magnetic scattering.

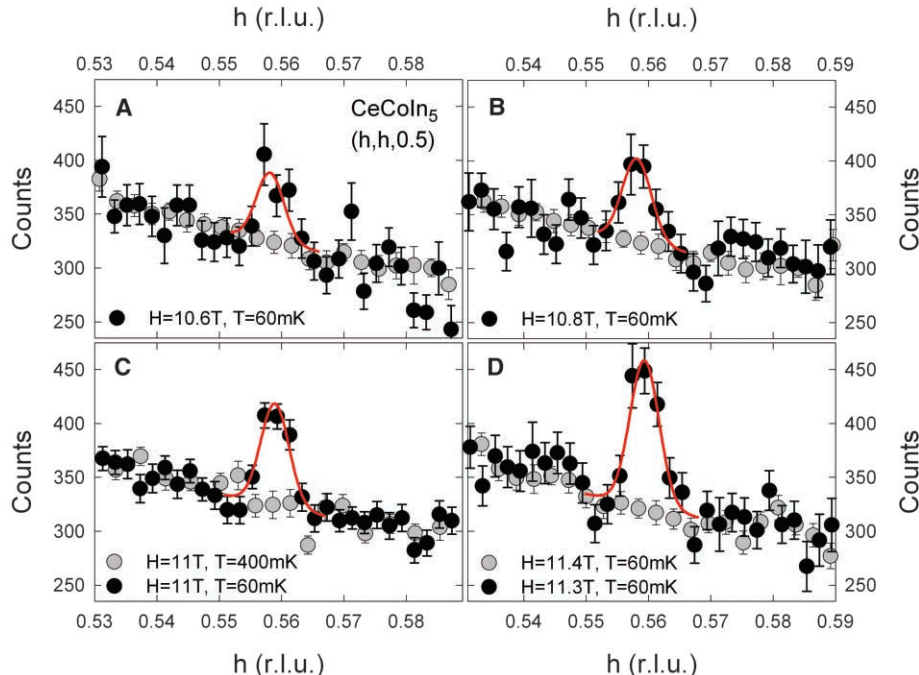
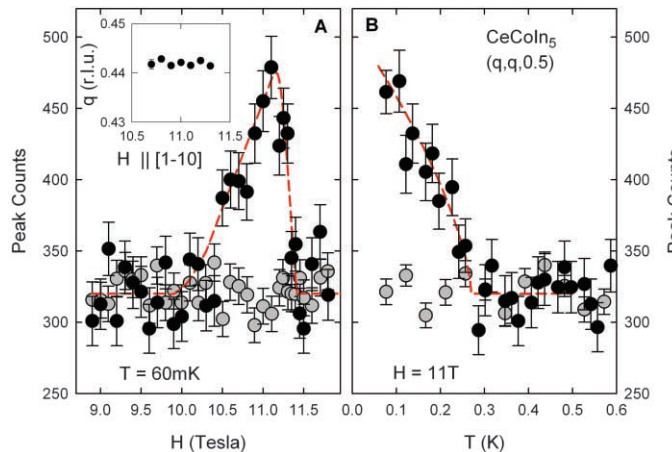


Fig. 3. Neutron-scattering intensity at $(q, q, 0.5)$, (A) as a function of field at $T = 60$ mK and (B) as a function of temperature at $H = 11$ T. The gray circles represent the background scattering taken from the two nearest to the center channels of the psd. The dashed red line in (A) is a guide to the eye, whereas the dashed line in (B) describes the background and the onset of the magnetic order in a second-order phase transition with $\beta = 0.365$ fixed to the critical exponent of the three-dimensional Heisenberg universality class. The inset shows that the q is field-independent.



The intimate link between superconductivity and magnetic order in CeCoIn₅ suggests the presence of a specific coupling between these order parameters (23). The multicomponent magnetosuperconducting phase can be reached via two second-order phase transitions through a suitable path in the H - T phase diagram, which justifies the construction of a phenomenological Landau coupling theory. If one assumes that the superconducting gap at zero field Δ_d has d_{x2-y2} symmetry, the possible coupling terms for magnetic fields in the basal plane that preserve time-reversal symmetry and conserves momentum can be written as $V_1 = \Delta_d^* M_q (H_x \Delta_{y,-q}^{(5)} + H_y \Delta_{x,-q}^{(5)}) + c.c.$, $V_2 = \Delta_d^* M_q (H_x D_x - H_y D_y) \Delta_{-q}^{(2)} + c.c.$, and $V_3 = \Delta_d^* M_q (H_x D_y - H_y D_x) \Delta_{-q}^{(3)} + c.c.$. Here, $(\Delta_{x,-q}^{(5)}, \Delta_{y,-q}^{(5)})$ belongs to the two-component even-parity Γ_5^+ state, $\Delta_{-q}^{(2)}$ and $\Delta_{-q}^{(3)}$ are the Γ_2^- and Γ_3^- odd-parity states (24), *c.c.* stands for the complex conjugate of the preceding term, and M_q is the magnetic-order parameter. These additional superconducting order parameters include a finite momentum $-q$. (D_x, D_y) is the gauge invariant gradient. Introducing the magnetic field allows one to couple M_q in linear order to preserve time-reversal symmetry. These combinations allow for a second-order phase transition within the superconducting phase and a first-order transition to the nonmagnetic normal state. For the coupling term V_2 , no magnetic structure is induced for fields $H \parallel [100]$. Given the weak dependence of the \mathbf{Q} phase on the magnetic field orientation in the basal plane, our measurements suggest the presence of a V_1 or V_3 coupling term, inducing the finite-momentum even-parity Γ_5^+ state or the odd-parity Γ_3^- state.

This Landau theory shows that incommensurate magnetic order induces a superconducting gap function that carries a finite momentum—the first experimental evidence of a superconducting condensate that carries a momentum. However, we show that this state may not arise purely from Pauli paramagnetic effects and the formation of a new pairing state between exchange-split parts of the Fermi surface, a state commonly known as the FFLO state (16, 17). In the FFLO state, the

pairing state carries a momentum of the Cooper pair that depends on the magnetic field via $|q| = 2\mu_B H/\hbar v_F$, where v_F is the Fermi velocity. However, the inset of Fig. 3A shows that $|q|$ is field-independent in CeCoIn₅, at odds with this prediction, which indicates that an additional superconducting pairing channel with finite momentum is induced in conjunction with the cooperative appearance of magnetic order.

A superconducting order that carries momentum illustrates the wealth of quantum phases that can exist in solid matter. The important microscopic role of magnetic fluctuations in the formation of Cooper pairs in CeCoIn₅ is self-evident because superconductivity emerges at $H_{c2}(0)$ simultaneously with ordered magnetism.

References and Notes

1. C. Petrovic *et al.*, *J. Phys. Condens. Matter* **13**, L337 (2001).
2. A. D. Bianchi, R. Movshovich, I. Vekhter, P. G. Pagliuso, J. L. Sarrao, *Phys. Rev. Lett.* **91**, 257001 (2003).
3. J. Paglione *et al.*, *Phys. Rev. Lett.* **91**, 246405 (2003).

4. K. Iizawa *et al.*, *Phys. Rev. Lett.* **87**, 057002 (2001).
5. N. J. Curro *et al.*, *Phys. Rev. B* **64**, 180514 (2001).
6. R. Movshovich *et al.*, *Phys. Rev. Lett.* **86**, 5152 (2001).
7. A. Vorontsov, I. Vekhter, *Phys. Rev. Lett.* **96**, 237001 (2006).
8. D. Hall *et al.*, *Phys. Rev. B* **64**, 212508 (2001).
9. R. Settai *et al.*, *J. Phys. Condens. Matter* **13**, L627 (2001).
10. A. D. Bianchi *et al.*, *Phys. Rev. Lett.* **89**, 137002 (2002).
11. A. D. Bianchi, R. Movshovich, C. Capan, P. G. Pagliuso, J. L. Sarrao, *Phys. Rev. Lett.* **91**, 187004 (2003).
12. A. D. Bianchi *et al.*, *Science* **319**, 177 (2008).
13. K. Kakuyanagi *et al.*, *Phys. Rev.* **94**, 047602 (2005).
14. T. Watanabe *et al.*, *Phys. Rev. B* **70**, 020506 (2004).
15. H. A. Radovan *et al.*, *Nature* **425**, 51 (2003).
16. P. Fulde, R. A. Ferrell, *Phys. Rev.* **135**, A550 (1964).
17. A. I. Larkin, Y. N. Ovchinnikov, *Sov. Phys. JETP* **20**, 762 (1965).
18. P. Monthoux, D. Pines, G. G. Lonzarich, *Nature* **450**, 1177 (2007).
19. J. Flouquet *et al.*, *C. R. Phys.* **7**, 22 (2006).
20. B. L. Young *et al.*, *Phys. Rev. Lett.* **98**, 036402 (2007).
21. Materials and methods are available as supporting material on *Science Online*.
22. C. Stock, C. Broholm, J. Hudis, H. J. Kang, C. Petrovic, *Phys. Rev. Lett.* **100**, 087001 (2008).
23. A. Aperis, G. Varelogiannis, P. B. Littlewood, B. D. Simons, *J. Phys. Cond. Mat.*, in press; preprint available at http://arxiv.org/PS_cache/arxiv/pdf/0804/0804.2460v1.pdf.
24. M. Sigrist, K. Ueda, *Rev. Mod. Phys.* **63**, 239 (1991).
25. Work at ETH was supported by the Swiss National Science Foundation under contract PP002-102831. This work is based on experiments performed at the Swiss spallation neutron source SINQ, Paul Scherrer Institute, Villigen, Switzerland, and was supported by the Swiss National Center of Competence in Research program Materials with Novel Electronic Properties. Work at Los Alamos was performed under the auspices of the U.S. Department of Energy and supported in part by the Los Alamos Laboratory Directed Research and Development program. A.D.B. received support from the Natural Sciences and Engineering Research Council of Canada (Canada), Fonds Québécois de la Recherche sur la Nature et les Technologies (Québec), and the Canada Research Chair Foundation.

Supporting Online Material

www.sciencemag.org/cgi/content/full/1161818/DC1

Materials and Methods

References

16 June 2008; accepted 7 August 2008

Published online 21 August 2008;

10.1126/science.1161818

Include this information when citing this paper.

Shape Changes of Supported Rh Nanoparticles During Oxidation and Reduction Cycles

P. Nolte,¹ A. Stierle,^{1*} N. Y. Jin-Phillipp,¹ N. Kasper,¹ T. U. Schulli,² H. Dosch¹

The microscopic insight into how and why catalytically active nanoparticles change their shape during oxidation and reduction reactions is a pivotal challenge in the fundamental understanding of heterogeneous catalysis. We report an oxygen-induced shape transformation of rhodium nanoparticles on magnesium oxide (001) substrates that is lifted upon carbon monoxide exposure at 600 kelvin. A Wulff analysis of high-resolution *in situ* x-ray diffraction, combined with transmission electron microscopy, shows that this phenomenon is driven by the formation of a oxygen–rhodium–oxygen surface oxide at the rhodium nanofacets. This experimental access into the behavior of such nanoparticles during a catalytic cycle is useful for the development of improved heterogeneous catalysts.

Many industrial chemicals and fuels are synthesized with the use of heterogeneous, solid-phase catalysts that often

contain metals in the form of nanoparticles (NPs). The direct study of these catalysts is challenging, and model catalysts such as single crys-